Veuve, N., Sychterz, A. and Smith, I.F.C. "Adaptive control of a deployable tensegrity structure", Engineering Structures, Vol 152, 2017, pp 14-23. doi.org/10.1016/j.engstruct.2017.08.062

Adaptive control of a deployable tensegrity structure

Nicolas Veuve[b], Ann C. Sychterz[a,*], Ian F.C. Smith[a]

[a] *Applied Computing and Mechanics Laboratory (IMAC), School of Architecture, Civil and Environmental Engineering (ENAC), Swiss Federal Institute of Technology (EPFL), CH-1015 Lausanne, Switzerland*
[b] *Emch + Berger SA Lausanne, Consulting Engineers, Ch. d'Entre-bois 26, CH-1008 Lausanne, Switzerland*

Abstract

Deployable structures belong to a special class of moveable structures that are capable of form and size change. Controlling movement of deployable structures is important for successful deployment, in-service adaptation and safety. In this paper, measurements and control methodologies contribute to the development of an efficient learning strategy and a damage-compensation algorithm for a deployable tensegrity structure. The general motivation of this work is to develop an efficient bio-inspired control framework through real-time measurement, adaptation, and learning. Building on previous work, an enhanced deployment algorithm involves re-use of control commands in order to reduce computation time for mid-span connection. Simulations are integrated into a stochastic search algorithm and combined with case-reuse as well as real-time measurements. Although data collection requires instrumentation, this methodology performs significantly better than without real-time measurements. This paper presents the procedure and generally applicable methodologies to improve deployment paths, to control the shape of a structure through optimization, and to control the structure to adapt after a damage event.

Keywords: Tensegrity structure, active control, deployable structures, adaptation

1. Introduction

Although active control of civil engineering structures has been studied for decades, few control strategies have been practically implemented. The first analytical study of active control of tall buildings involved mitigating effects of strong winds Yao (1972). For practical reasons involving control-system maintenance, active control for serviceability aspects is more feasible than long-return-period events such as earthquakes, as observed by Shea and Smith (1998).

Tensegrity structures, examples of space structures, are a system of struts and cables where mechanisms are stabilized by self-stress as discussed by Schenk et al. (2007) and Pellegrino and Calladine (1986). Interest in active control began to increase at the end of the

*Corresponding author. Address: EPFL ENAC IIC IMAC, Station 18, CH-1015 Lausanne, Switzerland. Phone number: +41 21 693 63 72

Email address: ann.sychterz@epfl.ch (Ann C. Sychterz)

last century, as discussed by Kawaguchi et al. (1996). These structures are good platforms to study active control as demonstrated in research by Tibert (2003) and Djouadi et al. (1998). Several patents have been submitted following work by Emmerich (1964), Fuller (1962), and Snelson (1965). Major theoretical and practical contributions for tensegrity structures include work by Motro (1992) Pellegrino (1990), and Skelton et al. (2001). More recent work on structural control of tensegrity structures was carried out by Zhang et al. (2014) on active cable-controled tensegrity structures and Sabouni-Zawadzka and Gilewski (2014) on control of a tensegrity plate after damage.

Tensegrity structures used as moving robots have been proposed by Paul et al. (2006). In robotics, these structures have compliancy requirements in order to reduce dynamic effects during movement. Structures in civil engineering applications are subject to more demanding requirements, such as minimum levels of stiffness to limit deflections.

A deployable structure, defined by Pellegrino (2001), typically changes shape in order to change size. The concept of a structure that changes shape has been proposed over forty years ago, see Zuk (1968). A scissor-like element by Gantes et al. (1989), bars in an X-shape pinned at their ends and midpoints, is an example of a structure that deploys along one degree of freedom. Simple deployable structures also include masts, solar arrays, and antennas such as those by Furuya (1992) and Tibert (2002). More recently, Kmet and Mojdis (2014) studied the stress development in an active-cable dome structure. Deployment along multiple degrees of freedom, which has not been extensively studied, is significantly more challenging to analyze and control compared with deployment along one degree of freedom.

Deployment of a large space mast used tape-spring hinges by Seffen and Pellegrino (1999). Xie et al. (2015) later studied iterative learning on a similar structure. Kmet and Platko (2014a) and Kmet and Platko (2014b) experimentally tested geometrical adaptation and pre-stress properties of a tensegrity module. When subjected to an external load, a control algorithm using a closed-form solution was analytically determined. Although active control of tensegrity structures has been the subject of these studies, only small deformations have been involved.

The concept of path planning has been applied by Rovira and Tur (2009) to a robot on a flat surface and a spherical robot on complex surfaces by Caluwaerts et al. (2014) and Bliss et al. (2013). Xu et al. (2014) developed path planning for object avoidance for accurate repeatable deployment. Damage compensation and shape adjustments have already been developed and tested in the field of self-repairing robotics. Several systems applied these concepts for digital replication and repair machines, autonomous repair, and self-reconfiguration of a modular system such as those studied by Mange et al. (1999), Huston et al. (2011), and Murata et al. (2001). Actuated structures permit slenderness ratios not otherwise possible such as the cantilever truss by Senatore et al. (2015). The structure computes nodal position based on element strain values and adapts to restore its initial position.

Control algorithms proposed by Aldrich and Skelton (2003) included minimum-time reconfiguration of tensegrity structures. Sultan (2014) proposed a nonlinear feedback cable-controled algorithm for tensegrity deployment. Path optimization and strut self-collision detection were studied by Le Saux et al. (2004) and real-time tests were conducted on a

movable tensegrity structure by Cefalo and Mirats Tur (2010). Although transformable tensegrities have been subjected to path optimization and collision detection studies, continuous monitoring has not been extensively used for subsequent improvement of performance.

Stiffness control was studied by Pinaud et al. (2004) on scaled tensegrity structures throughout deployment by manipulating tendons. A deployable tensegrity boom for space applications by Tibert (2003) has been built and tested where direction of deployment was parallel to gravity forces by Furuya (1992). Moored and Bart-Smith (2009) proposed a method to reduce the number of actuators for effective control of two and three-dimensional tensegrity structures using clustered elements. Clustered elements, applied in subsequent studies, also reduced the energy needed to accelerate the structure.

Adam and Smith (2008) showed that control of a tensegrity structure benefitted from reinforcement learning for self-diagnosis and multi-objective commands. Form-finding for the structure implemented dynamic relaxation (DR). Dynamic relaxation is a vector-based method that uses a pseudo-dynamic equilibrium to solve the static equilibrium form and forces of a structure by Barnes (1988). Day (1965) and Otter (1965) were early applications of DR in structural engineering. Inclusion of kinetic damping to improve convergence was proposed by Barnes (1988). Solutions for shape control of structures built upon the stochastic search algorithm, Probabilistic Global Search Lausanne (PGSL) which was conceived by Raphael and Smith (2003) and applied first to tensegrity control by Fest et al. (2004). This algorithm is based on the assumption that better sets of solutions are in the neighbourhood of good sets of solutions. The search space is sampled and a probability of finding a better solution is initially set to a constant value of the search space. Domer and Smith (2005) showed that implementing case-based re-use of control commands, a tensegrity structure was able to learn to react faster. Control movements did not involve deployment.

A "hollow-rope" tensegrity structure by Motro et al. (2006) was demonstrated to be suitable for a footbridge application using four identical connected pentagonal ring modules by Rhode-Barbarigos et al. (2010). Feasibility of deploying a near-full-scale tensegrity footbridge was shown by Veuve et al. (2015). Primarily due to variations in node behavior, the deployed position observed had up to 28 mm of variation for the same control command. This underscores the importance of testing near-full-scale structures; small models cannot represent full-scale realities.

Control of active cables has enabled successful connection at mid-span by Veuve et al. (2016). Building on previous achievements, the goal of the work described in this paper is to show effectiveness of adaptive control for i) improvement of deployment performance over time, ii) adaptation of the deployed structure due to damage and iii) in-service behavior improvements using measurements. The general motivation of this research is to develop efficient bio-inspired control algorithms for complex structures through the processes of learning, detection, and adaptation.

This paper addresses several research gaps outlined in the work reviewed above. Firstly, deployment over multiple degrees of freedom has not been extensively studied. Additionally, challenging deployment tasks have not often been tested on near-full-scale structures. Studies regarding active control of tensegrity structures have only involved small deformations. Lastly, aside from previous work by Adam and Smith (2007), no experimental study of active

control for damage compensation in civil structures was found.

Building on the previous work by Veuve et al. (2016), this paper includes descriptions and evaluations of adaptive control strategies for performance improvement and damage compensation through combining simulations, stochastic search and real-time measurements on a deployable tensegrity structure. Following a description of background research, re-use of previous control command sequences for mid-span connection of the two bridge halves is evaluated experimentally. Two methods for shape and stiffness enhancement using measurements are then compared. Lastly, a method for shape correction after damage is proposed and tested after removal of a non-continuous cable.

2. Background

This section provides a description of the laboratory structure and previous work on active control. Figure 1 a) shows a schematic of the elevation and Figure 1 b) shows a schematic of the cross-section of the full-scale structure used as a footbridge.

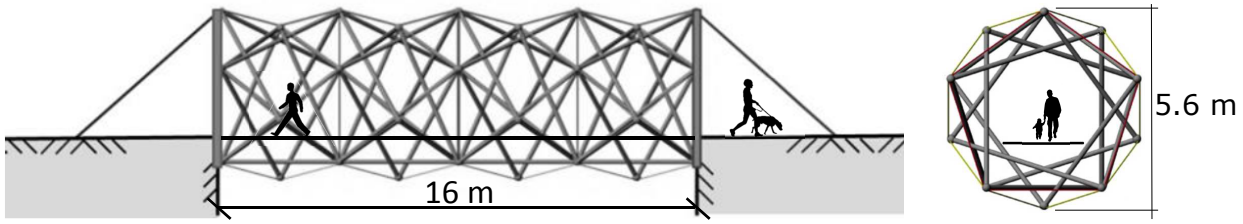

(a) (b)

Figure 1: Elevation view (a) and cross-section view (b) of a "hollow-rope" tensegrity footbridge concept by Motro et al. (2006)

A 1/4-scale model has been built in two halves that connect together at mid-span (Figure 2). A top view of the bridge in its folded configuration is given in Figure 2 a) and Figure 2 b) shows a similar view of the structure when connected. Each half includes fifteen low stiffness (spring) elements, twenty non-continuous cables, thirty struts, and five continuous active cables. A non-continuous cable is one segment of cable between two nodes. A continuous cable has at least one intermediate sliding contact point along its length between its terminal nodes. All continuous cables start from motors at the support nodes and end at the mid-span nodes. The actuation motors of continuous cables at the supports are installed on rail-supports. Rail-supports allow nodes to slide as deployment and folding cause changes in width and height of the structure.

Struts have a length of 1.35 m, a diameter of 28 mm, a thickness of 1.5 mm, a cross section of 11 mm^2 and they are fabricated from S355 grade steel as stated by Bel Hadj Ali et al. (2010). Cables are 3 mm diameter and fabricated from stainless steel. Spring elements have a stiffness of 2 kN/m at the supports and 2.9 kN/m otherwise. Each half of the bridge weighs approximately 100 kg. A tensegrity structure needs at least one state of self-stress to be stable. The number of independent self-stress states has been calculated using an extension of Maxwell's rule by Pellegrino and Calladine (1986) for determinacy in truss

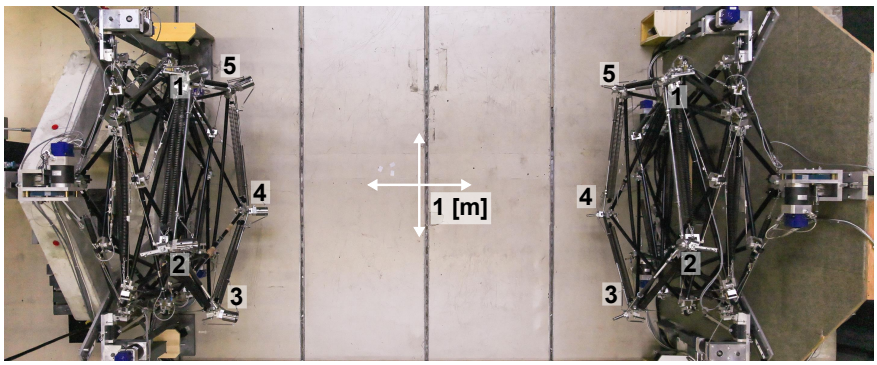

(a)

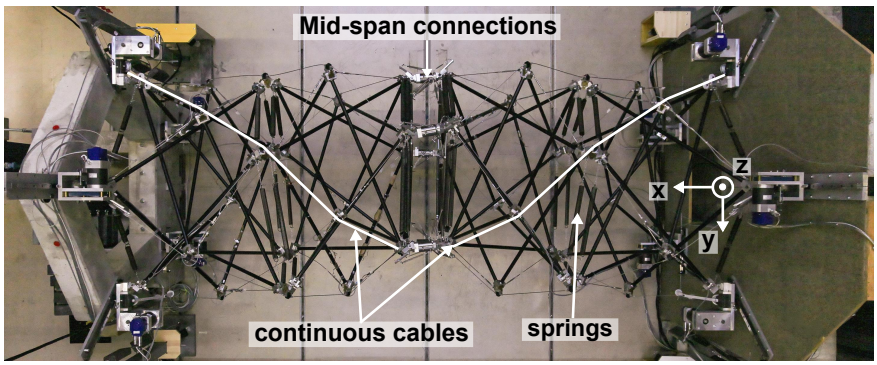

(b)

Figure 2: Top view of (a) folded structure showing the numbering of mid-span nodes and (b) deployed and connected structure at 1/4-scale (Figure 1) at mid-span, including x,y, and z directions.

structures. Tensegrity structures may have internal mechanisms where elongation is of a lower order compared with displacements. Also, the structure is geometrically nonlinear and thus traditional stiffness matrix inversion and superposition is not possible. The tensegrity structure with continuous cables has one state of self-stress and no mechanisms. More detail is in Veuve et al. (2015).

The structure measures 4 m in length, 1.5 m in height and 1.5 m in width and the interior space is intended for pedestrian passage, see Figure 1. Serviceability criteria for vertical deflection and resonance (1 Hz to 4.5 Hz) by Veuve et al. (2016) have been established for the structure when two halves of the bridge are connected and pre-stressed. Safety criteria for internal forces have been limited to below cable and spring tensile strength as well as below strut buckling loads. Due to the self-weight of the structure, connecting node pairs are joined sequentially.

The effect of the application of cable-length changes (control commands) on the structure is computed through numerical analysis using dynamic relaxation (DR) that has been adapted for continuous cables as proposed by Bel Hadj Ali et al. (2011) and Veuve et al. (2015). This adaptation involved requiring that all cable segments of continuous cables adopt the same tension values, thus assuming frictionless intermediate contact points. Domer et al. (2003) implemented DR within cycles that used the stochastic search algorithm (PGSL) to find good control comamands. This procedure was also used by Adam and Smith (2007).

Veuve et al. (2016) proposed two types of control commands (initial and additional) for the execution of the mid-span connection. Command solutions are evaluated by applying the cable length changes obtained from the stochastic search algorithm (PGSL) to the numerical model of the structure. The objective function is to minimize the distance between connecting nodes. To improve convergence, commands are limited to cable-length changes less than 10 mm per search step. Positions of connecting node pairs are measured to either determine if the nodes are connected or to update subsequent search cycles. If the connecting node pair is within the connection cone of diameter 30 mm, search terminates since connection is possible and the control commands are executed.

Additional control commands are cable length changes of 10 mm per step obtained from position measurements of all connecting nodes. Performance of each possible cable-length change combination is evaluated on its advancement towards nodal connection. The search for an additional control command requires testing several cable-length changes (five cable-length increases, five cable-length decreases). This is active control since cable-length changes are determined following measurements of strain and position using sensors on the structure. More detail is provided in Veuve et al. (2016).

This paper describes new methods that build on previously developed initial and additional control commands to achieve three goals. The first is to improve upon calculation times for midspan connection with re-use of control commands. The second goal is to control the stiffness and shape of the deployed structure. Lastly, initial and additional control commands are used for adaptation of the structure after damage.

3. Re-use of previous control commands for mid-span connection

Since the process of executing initial and additional control commands required long computational times (approximately 25 minutes using current control and computation hardware) several mid-span connection tests have been performed to accumulate cases. Due to unpredictable joint behavior arising from cable friction and node eccentricities, the structure does not deploy the same way twice using the same control commands Veuve et al. (2015). Also, nonlinearity means that closed-form solutions for cable-length changes to achieve mid-span connection of this structure are not available. Initial control commands using PGSL to search for the optimal cable length change are stored. In order to reduce the time spent during additional-control-command search, cases of additional control commands are stored and re-used.

The total cable-length changes over the duration of additional control commands have been combined into the cumulative mean over several tests. The cumulative mean for each cable then becomes the set of initial control commands for the next deployment event (see Figure 3). Using cumulative means of previous commands approximate best set of commands to use in a new situation when joint behavior is difficult to predict. If successful midspan connection is not possible, then additional control commands are computed using stochastic search based on relative position information of the connecting nodes.

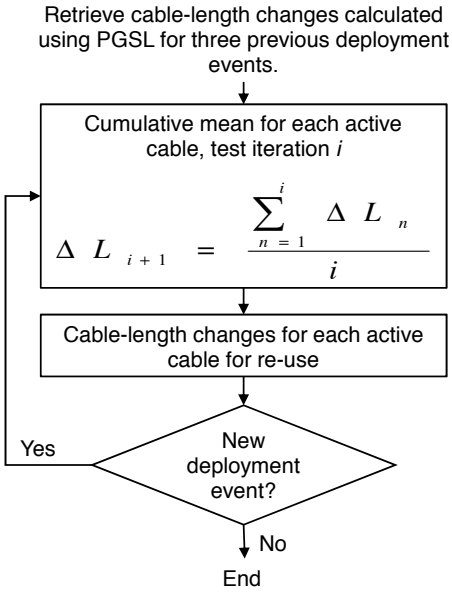

Figure 3: Cable-length changes and cumulative mean of each active cable for re-use.

Deployment, folding, and actuation of the structure occurs due to energy storage in the springs and length changes of the continuous cables at a slow speed where inertial effects can be ignored. Veuve et al. (2015) observed a maximum nodal-position difference of 28 mm following multiple cycles of folding and deployment. Of the elements with strain gauges, the percent difference between the maximum and the mean of peak element force values

over several cycles of deployment are 2% for struts, 4% for discontinuous cables, and 1% for continuous cables studied by Veuve (2016). Given a reliability of 95%, these values do not exceed the given threshold for statistical significance. Thus strain measurements are poor indicators of deployed position variations.

The mean deflection at mid-span prior to connection is approximately 315 mm, thus a maximum mid-span node variation (28 mm) results in a 9% deflection variation. Full-scale structures subjected to environmental effects would demonstrate similar variability. Self-weight of the structure also influences the deflection. Additionally, at mid-span prior to connection is the location where lowest cable stiffness values occur. Therefore, this structure provides an opportunity to develop control strategies that are suitable for field conditions.

Figure 4 shows additional control commands (Section 2) applied for the connection of a node during three tests. All tests have led to successful connections. The magnitudes of cable length changes vary among the tests. Control command variation is due to the non-repeatable behavior of the structure and the error related to the measurement precision. The third test is the best since it requires less cable-length change.

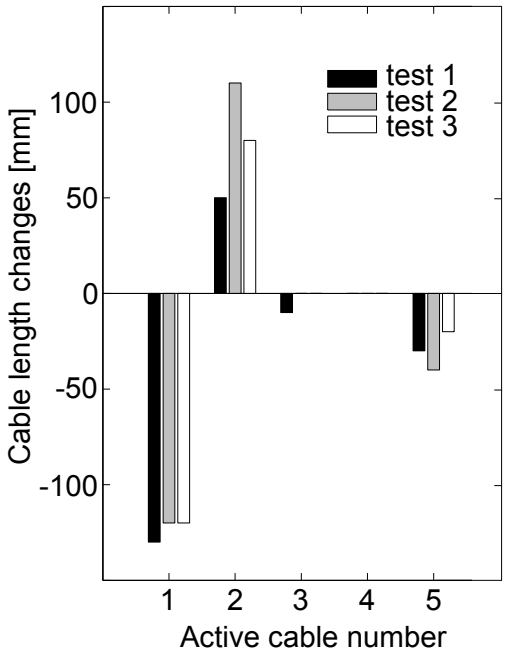

Figure 4: Comparison of total cable-length changes applied in three connection tests on laboratory structure, for connection of mid-span Node 3

Evolution of distance between connecting nodes of a mid-span Node 3 is shown in Figure 5. The control-command cases that are re-used in the first twenty-seven steps are mean values of the commands obtained in the first three mid-span connection tests. Figure 5 a) shows the distance along the axis of the footbridge (x axis) and Figure 5 b) the distance in the plane perpendicular to the axis of the footbridge (yz plane). The vertical dotted lines indicate the step where the connection between the two parts of Node 3 is initiated using

additional control commands. Twelve steps are required before initiation of the connection and twenty-nine steps for the full connection of the two node parts. Figure 5 b) demonstrates that the distance at connection initiation is less than the 30 mm tolerance of misalignment between both parts of the connection node. The 20 mm distance in the yz plane remaining at full connection reveals that when connected, the mid-span node is not aligned with the axis of the footbridge.

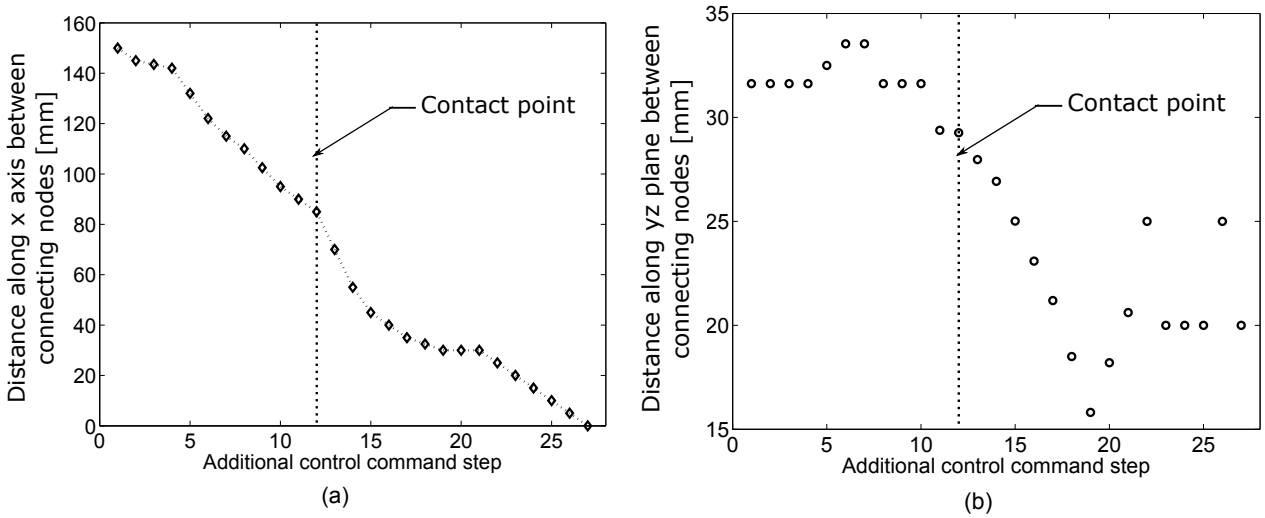

Figure 5: Sample of experimental results of the distance (a) along the x-axis between two connecting parts of Node 3 [mm] and (b) between two connecting nodes [mm] in the yz-plane. Point of contact between joining structure halves shown with a vertical dotted line.

Table 1 shows the number of additional control commands searched and re-used for all five connections during five mid-span connection tests. The time spent for finding additional control commands is indicated in the last column. Application of previous commands followed by search is approximately ten times faster than searching a new command without re-use. This confirms that this strategy, originally proposed by Domer and Smith (2005) for small-scale shape control is appropriate for deployment shape control.

4. Enhancement of in-service performance

This section describes the methodologies for adaptation based on stiffness control and shape control of the structure. The in-service state is defined as the structure in a connected and self-stressed state. Adaptation due to load or a damaged element are the performance goals while the structure is in this state.

4.1. Stiffness control

Two methodologies are presented for stiffness control: the first based on simulated values only, and the second based on comparing simulation results with measurement data. Stiffness

Table 1: Number of additional control commands for connection of each mid-span node during three training tests and re-use of control command followed by search during a fourth and fifth test

Mid-span connection test number	Origin of control commands	Mid-span node					Time [min]	Total time [min]	Normalized time
		1	2	3	4	5			
1	search	0	4	22	0	5	23	23	0.8
2	search	0	5	27	0	10	29.5	29.5	1
3	search	0	10	22	0	7	27.5	27.5	0.9
4	re-use	0	10	27	0	7	1.5		
	search	1	0	2	0	0	2	3.5	0.1
5	re-use	0	10	29	0	7	1.5		
	search	0	0	1	0	0	0.66	2.2	0.1

of the footbridge as a critical aspect since the structural design is governed by the deflection criterion by Rhode-Barbarigos et al. (2012). Stiffness is determined through applying load to the structure and measuring the change in deflection. The vertical displacement is measured during two loading events for both cases. Average displacements are used to estimate the stiffness of the structure.

In both methodologies, the output of PGSL is cable-length changes; they are then used as input for DR simulations. Equilibrium configurations after cable-length changes and loading are calculated sequentially. The constraint of the objective function involves a comparison of the internal forces with element strength. The dynamic relaxation analysis accounts for all coupled and nonlinear behavior.

4.1.1. First methodology

The stochastic search and dynamic relaxation algorithms are employed within the first methodology as shown in Figure 6. The objective function value of stiffness in kN/m $OF_{1,stiff}$ is defined in Equation 1. Only the maximum value of the objective function is considered.

$$MAX\{OF_{1,stiff} = [load]/(z_{f,s} - z_{0,s})\} \tag{1}$$

Subject to:

$$|Nf_{d,i}| - 0.5 \cdot N_{Rd,i} < 0 \quad i = 1, ..., ne \tag{2}$$

The variable $z_{f,s}$ refers to the simulated (subscript s) vertical position of the lowest mid-span node after loading (subscript f). The variable $z_{0,s}$ refers to the simulated (subscript s) vertical position of the lowest mid-span node before loading (subscript 0). In this case, the loading is 1.5 kN.

Equation 2 is an optimization constraint that limits internal forces in elements. In this equation, ne refers to the number of elements in the structure and $N_{Rd,i}$ the element (subscript i) strength (tensile strength of cables and springs and buckling strength of struts). Simulated internal forces in elements are compared to element strengths. When internal forces due to the 1.5 kN load ($Nf_{d,i}$) exceed 50% of the element strength ($N_{Rd,i}$), for any

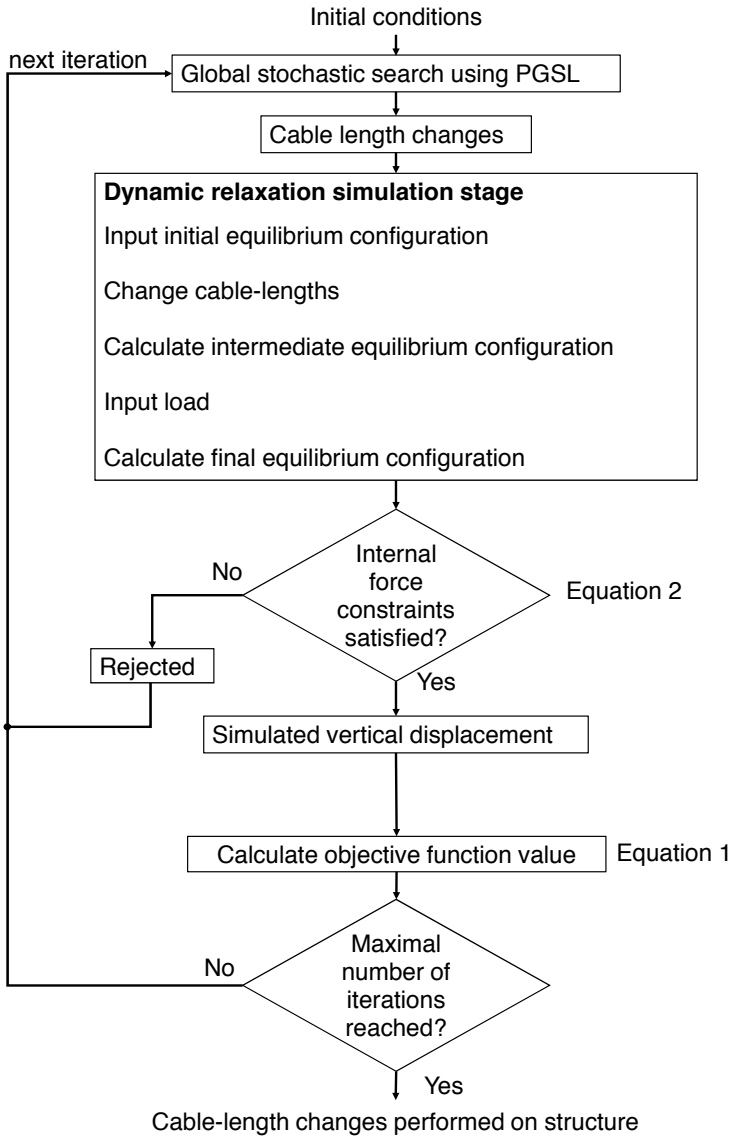

Figure 6: Enhancement of in-service performance for the first methodology. Cable-length changes modify objective-function values of vertical displacement [mm]

i, the constraint related to safety of the test is not satisfied, see Equation 2. A maximum internal force level of 50% of element strength is standard experimental practice. While practical situations may involve using other values, this limit is adopted for the purposes of this paper. Solutions exceeding the limits of Equation 2 are rejected.

Table 2 shows the simulated deflections at mid-span for two load cases. The lowest mid-span node moves more than the average value of all nodes. The deflection of this node when the structure is loaded is thus used to provide a stiffness metric.

Table 2: Simulated displacements at mid-span

Load case	Total load [kN]	Deflection at the lowest mid-span node [mm]	Average vertical deflection of all nodes [mm]
Distributed load	4	45	22
Concentrated at mid-span	1.5	31	18

4.1.2. Second methodology

Control solutions that are also found using PGSL are evaluated within the second methodology as described in Figure 7. The process is the same as for the first methodology until verification of internal forces. When the constraint is satisfied, cable lengths are changed on the structure and then the structure is loaded. Displacement due to the load is measured and returned to calculate the objective function value.

The objective function $OF_{2,stiff}$ for this second methodology employs the mean of the measured relative displacements of the mid-span node to calculate for stiffness in kN/m, see Equation 3. Only the maximum value of the objective function is considered.

$$MAX\{OF_{2,stiff} = [load]/\Big((z_{f,m1} - z_{0,m1}) + (z_{f,m2} - z_{0,m2})\Big)/2\} \tag{3}$$

The terms $z_{f,m1}$ and $z_{f,m2}$ are the measured vertical position of the lowest mid-span node after first and second load application, respectively. Similarly, the terms, $z_{0,m1}$ and $z_{0,m2}$, are the measured vertical positions of the lowest mid-span node after the first and second removal of load from the structure.

The second methodology leads to a reduction of approximately 50% of the deflection for the two tests. Figure 8 and Figure 9 show evolution of the deflection during iterations of stiffness enhancement using the second methodology. Figure 8 shows that the vertical deflection remains at a value of close to 10 mm for approximately 35 iterations. Although more iterations are performed in test results indicated in Figure 9, the deflection does not reach a smaller value than 13 mm.

4.1.3. Comparison of methodologies

A summary of stiffness enhancement attempts are given in Table 3. The first row indicates the performance of the structure subject to a 1.5 kN load at mid-span without stiffness

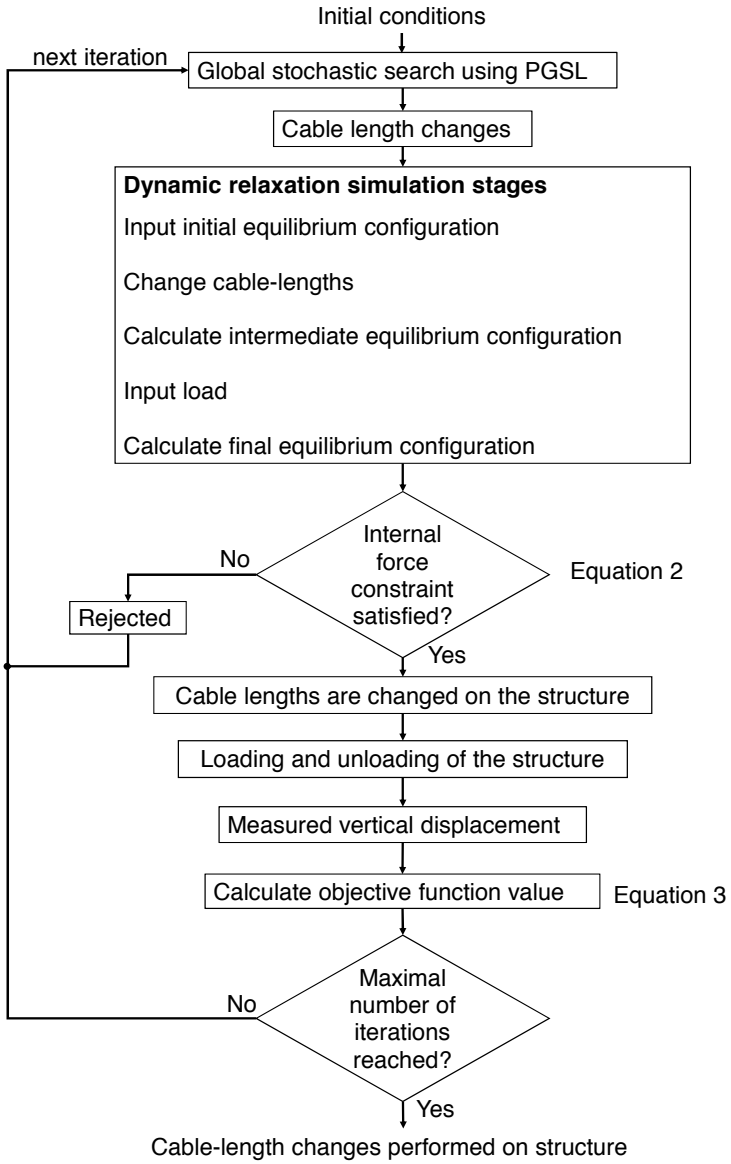

Figure 7: Enhancement of in-service performance for the second methodology. Determination of the objective function value using direct measurement of vertical displacement [mm]

control. Simulated and measured displacements due to the load are shown for all tests. Measured deflection at mid-span after application of a solution found with the first methodology results in measured performance that is worse than the no-control configuration. An adaptive methodology based on simulation alone is thus not effective for stiffness control of this structure.

Considering the low number of iterations involved in the two tests presented in Figure 8 and Figure 9, the best solutions found may not be a global optimum. Evaluation of the objective function with the second methodology is approximately ten times slower than with the first methodology. Nevertheless, stiffness is increased by an average of 44%.

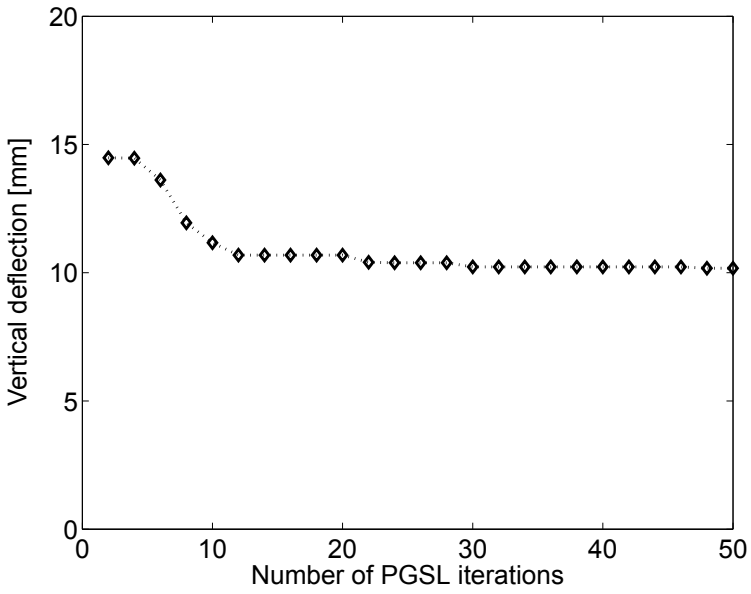

Figure 8: Convergence curve of the control command algorithm in the second methodology using response measurements from the laboratory structure in real-time during a fifty-iteration test

Table 3: Comparison of the two control methodologies

Type of control	Number of evaluations	Simulated deflection [mm]	Measured deflection [mm]
No control	-	15.6	20.2
First methodology	1000	8.7	28.8
Second methodology	50	16.9	10.2
Second methodology	100	16.1	12.6

Table 4 presents three additional solutions that have been obtained with the second methodology. Cable numbers correspond to the connecting nodes in Figure 2. Results of the first methodology are not shown. While values of the control commands differ, each solution performs similarly. This indicates the complexity of the solution space. Stiffness is increased by an average of 36%. Therefore, stiffness is successfully improved through cycles of loading

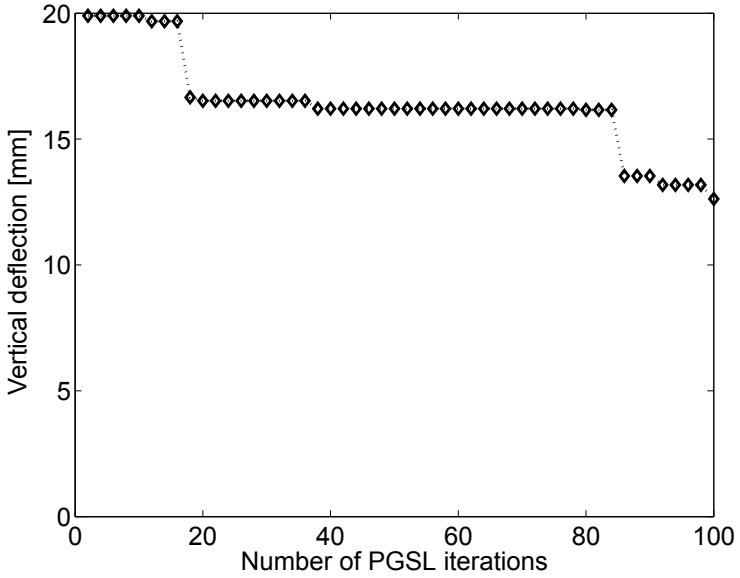

Figure 9: Convergence curve of the control command algorithm in the second methodology using response measurements from the laboratory structure in real-time during a 100-iteration test

and measurement. While the loading could be applied when commissioning a structure, this procedure would not be convenient for multiple deployment applications. Future work involves development of strategies to avoid initial loading cycles with pre-defined loads.

Table 4: Three sample solutions of the second methodology that result in similar deflections

Solution	Cable-length changes [mm]					Deflection[mm]	Stiffness enhancement (%)
	Cable 1	Cable 2	Cable 3	Cable 4	Cable 5		
1	-9.3	-6.9	2.4	14.2	1.2	12.7	37
2	-12.1	14	5.9	10.3	-9.6	12.6	38
3	-13.3	-13.2	14.1	10.1	-12.8	13.2	35

Figure 10 shows evolution of deflection during iterations using the second methodology. Each point in the graph is a position of the mid-span node that is measured on the structure. Since the distance is progressively reduced, the control system is able to adjust according to previous experience. However, after approximately 350 iterations, the target value is exceeded. Extension of the algorithm in order to reach solutions that converge within a tolerance range around the target is subject of future work.

4.2. Shape control after damage

Shape control is implemented to increase the vertical position of the lowest mid-span node of a damaged structure as close as possible to a desired height. For the purposes of this study, the desired height is defined as the position that the lowest mid-span node would

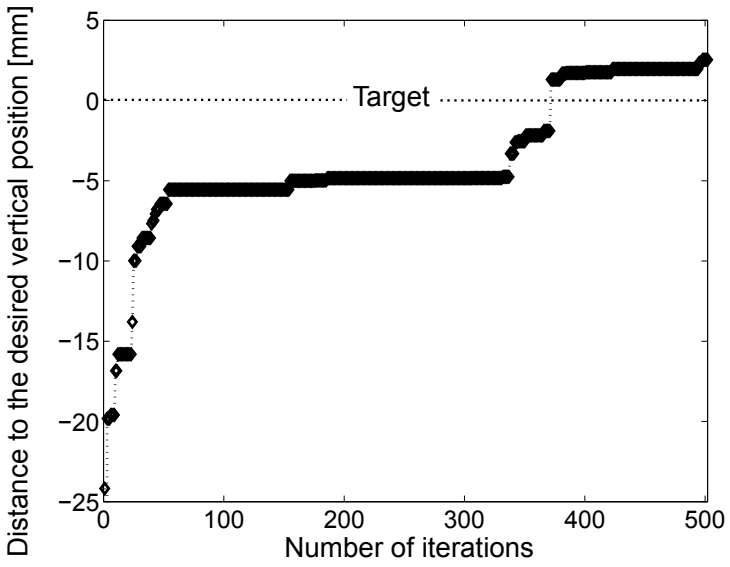

Figure 10: Convergence curve of shape control using the second methodology

take if the structure had zero self-weight. The damage location algorithms used to identify damaged elements is presented by Veuve et al. (2016), and are not in the scope of this paper.

When non-continuous cable damage occurs, the control system is able to detect damage occurrence and focus on possible damage locations. Damage of a non-continuous cable has been experimentally measured as the state of the structure before and after the uninstallation of a cable. Similar to the stiffness enhancement method, an objective function is defined for a correction strategy of cable-length changes. Possible damage locations are identified through comparison of simulations with measurements taking uncertainties into account. Several actuation events are performed in order to increase the number of useful measurements. Equation 4 shows the objective function for shape control. Only the minimum value of the objective function is considered.

$$MIN\{OF_{shape} = z_{desired,s} - z_{c,s}\} \tag{4}$$

Subject to:

$$|Ns_{d,i}| - 0.5 \cdot N_{Rd,i} < 0 \quad i = 1, ..., ne \tag{5}$$

The objective function OF_{shape} corresponds to simulated distance between the position of the lowest mid-span node after simulation of the control command $z_{c,s}$ and the desired position $z_{desired,s}$. In Equation 5, $Ns_{d,i}$ refers to the simulated internal forces in an element when the structure is subject to the self-weight load. When Equation 4 is not satisfied for any i, the solution is rejected. Cable damage, Figure 11, was tested and measured on the tensegrity structure.

4.2.1. Adaptation strategy

The goal of shape control after damage is to bring the position of the lowest mid-span node back to a desired position. Figure 12 describes the methodology for shape correction

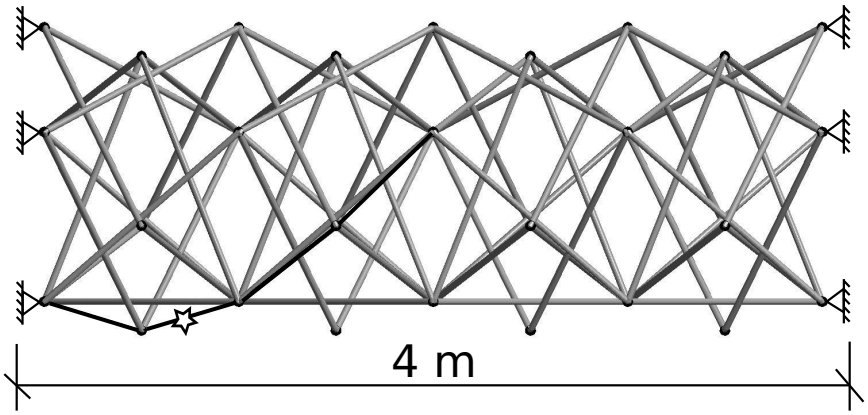

Figure 11: Elevation view of 1/4-scale deployed structure showing end conditions following prestress. The location of discontinuous cable damaged for testing is indicated by a star. For clarity, struts (in grey) and only some cable segments (in black) are shown.

after damage. Since diagnosis is a reverse engineering task, it results in identification of multiple damage scenarios (candidate scenarios) and therefore, all identified scenarios are taken into account in simulations of the structure. The internal force constraint, Equation 5, is imposed on all candidate scenarios. Uncertainties arise due to factors such as measurement, modeling, material strength, cable tension, and support stiffness. Given that uncertainties can be estimated and prioritized, this method can be successful to other tensegrity structures to identify possible damage locations.

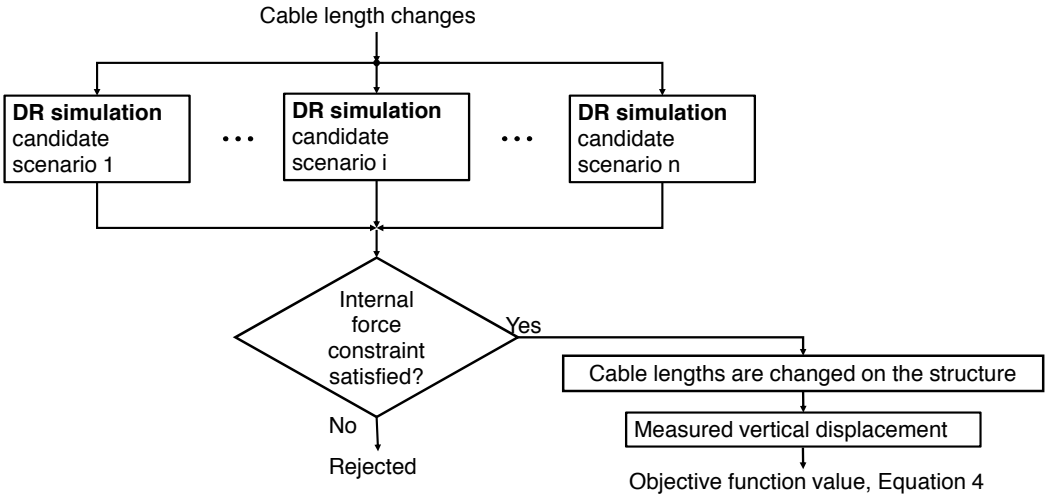

Figure 12: Control command search for damage adaptation

Control command search for damage adaptation uses real-time structural responses and damage diagnosis. Figure 13 shows the progression curve of shape control after damage for a 200-iteration test. The horizontal axis shows the number of iterations and the vertical axis shows the objective function value which is the distance to the desired position in mm. All

points in this graph are obtained from position measurement on the lowest mid-span node of the structure. This graph demonstrates that successful shape correction is achieved after a 200-iteration test. Therefore, the algorithm described in Figure 12 is able to converge on control commands for a desired shape correction adaptation after an element is damaged.

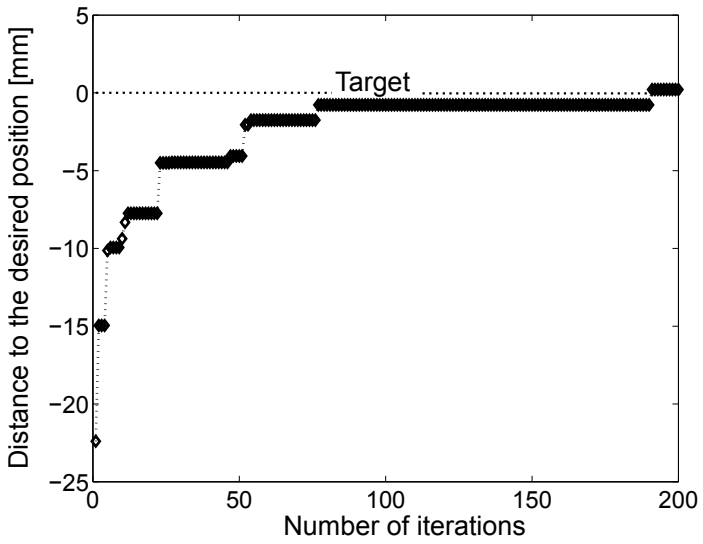

Figure 13: Damage adaptation using response measurements from the laboratory structure

Prediction of internal forces are performed in order to check whether or not internal forces exceed element strength. Average predicted cable tension values were approximately 1 kN. When predicted tension values were less than 1 kN, cables may be without tension on the structure. In all cases, predictions were greater than measured values, even during several deployment sequences. A simplified model that is based on dimensionless and frictionless nodes for assessing internal forces due to a potential control command prior to actuation is justified because test results show that predictions of element forces are conservative.

5. Discussion

During mid-span connection, re-use of previous control commands considerably reduces the time required to connect both bridge halves. Adaptation of a control command sequence is based on measurements after application of each previous control command. Application of previous commands followed by search is approximately ten times faster than searching a new command without re-use.

Control commands for stiffness and shape enhancement that are computed through a combination of stochastic search and simulations are not always successful. Of the two methodologies proposed for stiffness control, the second methodology, which uses measurements taken from the structure, is more successful than the first methodology, which uses simulated values only. Control commands successfully achieved the target position for shape

control of the structure when using a combination of measurements and simulations. Methods that do not use measurement data rely soley on simulation assumptions that may not be satisfied on the near full-scale structure. For example, non-dimensional and friction-free nodes are assumptions that do not correspond to reality.

Experimental measurements during control command application vary for each test even in laboratory conditions. Variations are likely due to uncertain deployment behavior and friction effects. Using measurement of the response in real-time helps account for these variations. This advantage would be even more important for a full-scale structure where changing environment conditions(temperature and wind) are likely. The drawback of implementing a methodology that combines measurements and simulated values is the additional computation time. Despite this, large-scale models of future large-displacements tensegrity structures will be necessary to understand their structural behavior.

Shape control using a comparison of measurements and scenarios of simulated values was successful to reduce mid-span deflection due to a damaged element. Internal forces of elements are calculated for all candidate scenarios identified during damage diagnosis. Convergence to a successful shape correction happens in a short amount of time, thus can be implemented in future adaptation algorithms for large-displacement tensegrity structures. Since these calculations over-estimate real behavior, resulting control commands will not over-stress the structure.

6. Conclusions

Compared with pre-defined control commands and second-stage optimized control as proposed in previous work, re-use of control-command sequences reduces search time during mid-span connection of a tensegrity structure and allows for adjustments guided by measurements.

A stochastic search algorithm that includes real-time measurements performs better than only simulations for stiffness and shape control. Active control contributes to incremental improvement since real-time measurements improve structural performance through use of measurement data in a adaptive control strategy.

The methodology described in this paper sucessfully determined control commands for a desired shape-correction adaptation after an element is damaged. The tensegrity structure does not deploy to the same position each time. Non-repeatable deployment is expected to be common in practical environments. Using this methodology, relatively simple models of the structure can be successfully combined with appropriate control commands. This strategy can be applied to other large-scale structures that deploy along many degrees of freedom, tensegrity or otherwise.

Damage adaptation with real-time measurements is successful and accommodates ambiguity due to multiple possible damage locations. A simplified model that is based on dimensionless and frictionless nodes is acceptable for verification of the tensegrity structure because test results show that predictions are conservative.

Acknowledgements

The research is sponsored by funding from the National Science Foundation under project number 20020_144305. The authors would like to thank Nizar Bel Hadj Ali, Seif Dalil Safaei and Landolf Rhode-Barbarigos for fruitful discussions.

References

Adam, B., Smith, I. F., 2008. Active tensegrity: A control framework for an adaptive civil-engineering structure. Computers & Structures 86 (23-24), 2215–2223.

Adam, B., Smith, I. F. C., 2007. Self-Diagnosis and Self-Repair of an Active Tensegrity Structure. Journal of Structural Engineering 133 (12), 1752–1761.

Aldrich, J. B., Skelton, R. E., 2003. Control/structure optimization approach for minimum-time reconfiguration of tensegrity systems. In: Smart Structures and Materials: Modeling, Signal Processing, and Control, 1st Edition. Vol. 5049. SPIE, San Diego, CA, USA, pp. 448–459.

Barnes, M. R., 1988. Form-finding and analysis of prestressed nets and membranes. Computers and Structures 30 (3), 685–695.

Bel Hadj Ali, N., Rhode-Barbarigos, L., Albi, A. A. P., Smith, I. F. C., 2010. Design optimization and dynamic analysis of a tensegrity-based footbridge. Engineering Structures 32 (11), 3650–3659.

Bel Hadj Ali, N., Rhode-Barbarigos, L., Smith, I. F., 2011. Analysis of clustered tensegrity structures using a modified dynamic relaxation algorithm. International Journal of Solids and Structures 48 (5), 637–647.
URL http://linkinghub.elsevier.com/retrieve/pii/S0020768310003914

Bliss, T., Iwasaki, T., Bart-Smith, H., 2013. Central pattern generator control of a tensegrity swimmer. Mechatronics, IEEE/ASME Transactions on 18 (2), 586–597.

Caluwaerts, K., Despraz, J., Işçen, A., Sabelhaus, A. P., Bruce, J., Schrauwen, B., SunSpiral, V., 2014. Design and control of compliant tensegrity robots through simulation and hardware validation. Journal of The Royal Society Interface 11 (98), 20140520.

Cefalo, M., Mirats Tur, J., 2010. Real-time self-collision detection algorithms for tensegrity systems. International Journal of Solids and Structures 47 (13), 1711–1722.

Day, A., 1965. An introduction to dynamic relaxation(dynamic relaxation method for structural analysis, using computer to calculate internal forces following development from initially unloaded state). The Engineer 219, 218–221.

Djouadi, S., Motro, R., Pons, J. C., Crosnier, B., 1998. Active Control of Tensegrity Systems. Journal of Aerospace Engineering 11 (4), 37–44.

Domer, B., Fest, E., Lalit, V., Smith, I. F., 2003. Combining dynamic relaxation method with artificial neural networks to enhance simulation of tensegrity structures. Journal of Structural Engineering 129 (5), 672–681.

Domer, B., Smith, I. F. C., 2005. An Active Structure that Learns. Journal of Computing in Civil Engineering 19 (1), 16–24.

Emmerich, D., 1964. Construction de réseaux autotendants. Ministere de l'industrie, France (Patent No. 1,377,290).

Fest, E., Shea, K., Smith, I. F. C., 2004. Active Tensegrity Structure. Journal of Structural Engineering 130 (10), 1454–1465.

Fuller, B., 1962. Tensile-integrity structures (US Patent No. 3,063,521, USA).

Furuya, H., 1992. Concept of deployable tensegrity structures in space applications. International Journal of Space Structures 7 (2), 143–151.

Gantes, C. J., Connor, J. J., Logcher, R. D., Rosenfeld, Y., 1989. Structural analysis and design of deployable structures. Computers and Structures 32 (3-4), 661–669.

Huston, D., Hurley, D., Gollins, K., Gervais, A., Ziegler, T., 2011. Damage Detection and Autonomous Repair System Coordination. Advances in Structural Engineering 14 (1), 41–45.

Kawaguchi, K.-I., Hangai, Y., Pellegrino, S., Furuya, H., 1996. Shape and stress control analysis of prestressed truss structures. Journal of Reinforced Plastics and Composites 15 (12), 1226–1236.

Kmet, S., Mojdis, M., 2014. Adaptive Cable Dome. Journal of Structural Engineering 141 (9), 1–16.

Kmet, S., Platko, P., 2014a. Adaptive tensegrity module. part 1: Closed-form and finite-element analyses. Journal of Structural Engineering 140 (9), 04014055.

Kmet, S., Platko, P., 2014b. Adaptive tensegrity module. part 2: Tests and comparison of results. Journal of Structural Engineering 140 (9), 04014056.

Le Saux, C., Cavaer, F., Motro, R., 2004. Contribution to 3d impact problems: Collisions between two slender steel bars. Comptes Rendus - Mechanique 332 (1), 17–22.

Mange, D., Sipper, M., Marchal, P., 1999. Embryonic electronics. BioSystems 51 (3), 145–152.

Moored, K., Bart-Smith, H., 2009. Investigation of clustered actuation in tensegrity structures. International Journal of Solids and Structures 46 (17), 3272–3281.

Motro, R., 1992. Tensegrity systems: the state of the art. International journal of space structures 7 (2), 75–83.

Motro, R., Maurin, B., Silvestri, C., 2006. Tensegrity rings and the hollow rope. In: IASS Symposium Beijing China.

Murata, S., Yoshida, E., Kurokawa, H., Tomita, K., Kokaji, S., 2001. Self-Repairing Mechanical Systems. Autonomous Robots 10, 7–21.

Otter, J., 1965. Computations for prestressed concrete reactor pressure vessels using dynamic relaxation. Nuclear Structural Engineering 1 (1), 61–75.

Paul, C., Valero-Cuevas, F. J., Lipson, H., 2006. Design and control of tensegrity robots for locomotion. IEEE Transactions on Robotics 22 (5), 944–957.

Pellegrino, S., 1990. Analysis of prestressed mechanisms. International Journal of Solids and Structures 26 (12), 1329–1350.
URL http://dx.doi.org/10.1016/0020-7683(90)90082-7

Pellegrino, S., 2001. Deployable Structures. Spring-Verlag Wien, Vienna.

Pellegrino, S., Calladine, C., 1986. Matrix analysis of statically and kinematically indeterminate frameworks. International Journal Solids Structures 22 (4), 409–428.

Pinaud, J.-P., Solari, S., Skelton, R. E., 2004. Deployment of a class 2 tensegrity boom. In: Smart Structures and Materials 2004: Smart Structures and Integrated Systems, 1st Edition. Vol. 5390. SPIE, San Diego, CA, USA, pp. 155–162.

Raphael, B., Smith, I. F. C., 2003. A direct stochastic algorithm for global search. Applied Mathematics and Computation 146, 729–758.

Rhode-Barbarigos, L., Ali, N., Motro, R., Smith, I., 2012. Design aspects of a deployable tensegrity-hollow-rope footbridge. International Journal of Space Structures 27 (2-3), 81–96.

Rhode-Barbarigos, L., Ali, N. B. H., Motro, R., Smith, I. F., 2010. Designing tensegrity modules for pedestrian bridges. Engineering Structures 32 (4), 1158–1167.

Rovira, A. G., Tur, J. M. M., 2009. Control and simulation of a tensegrity-based mobile robot. Robotics and Autonomous Systems 57 (5), 526–535.

Sabouni-Zawadzka, A. A., Gilewski, W., 2014. Control of Tensegrity Plate due to Member Loss. Procedia Engineering 91 (TFoCE), 204–209.
URL http://linkinghub.elsevier.com/retrieve/pii/S1877705814030653

Schenk, M., Guest, S., Herder, J., 2007. Zero stiffness tensegrity structures. International Journal of Solids and Structures 44 (20), 6569–6583.

Seffen, K. A., Pellegrino, S., 1999. Deployment dynamics of tape springs. Proceedings of the Royal Society of London A: Mathematical, Physical and Engineering Sciences 455 (1983), 1003–1048.

Senatore, G., Winslow, P., Duffour, P., Wise, C., 2015. Infinite stiffness structures via active control. In: Proceedings of the International Association for Shell and Spatial Structures 2016, Amsterdam, The Netherlands. pp. 1–12.

Shea, K., Smith, I., 1998. Intelligent structures: A new direction in structural control. In: Artificial Intelligence in Structural Engineering. Vol. 1454 of Lecture Notes in Computer Science. Springer Berlin Heidelberg, pp. 398–410.

Skelton, R. E., Adhikari, R., Pinaud, J.-P., Chan, W. L., 2001. An introduction to the mechanics of tensegrity structures. In: Conference on Decision and Control. Orlando, Florida, USA, pp. 4254–4259.

Snelson, K., 1965. Continuous tension, discontinuous compression structures (US Patent No. 3,169,611, USA).

Sultan, C., 2014. Tensegrity deployment using infinitesimal mechanisms. International Journal of Solids and Structures 51 (21-22), 3653–3668.

Tibert, A. G., 2003. Deployable tensegrity masts. In: Structures, Structural Dynamics, and Materials Conference and Exhibit. No. 4. pp. 1–10.

Tibert, G., 2002. Deployable tensegrity structures for space applications. Royal Institute of Technology.

Veuve, N., 2016. Towards biomimetic behavior of an active deployable tensegrity structure. Phd, Ecole polytechnique federale de Lausanne, Station 18, 1015 Lausanne, Switzerland.

Veuve, N., Dalil Safaei, S., Smith, I., 2016. Active control for mid-span connection of a deployable tensegrity footbridge. Engineering Structures 112, 245–255.

Veuve, N., Safaei, S., Smith, I., 2015. Deployment of a tensegrity footbridge. Journal of Structural Engineering 141 (11), 04015021–1–04015021–8.

Xie, Y., Xie, C., Shi, H., 2015. Deployment Process Control of Space Masts via Iterative Learning Control. In: The 27th Chinese Control and Decision Conference, Qingdao, China. pp. 1032–1037.

Xu, X., Sun, F., Luo, Y., Xu, Y., 2014. Collision-free path planning of tensegrity structures. Journal of Structural Engineering 140 (4).

Yao, J. T., 1972. Concept of structural control. Journal of the Structural Division 98 (7), 1567–1574.

Zhang, P., Kawaguchi, K., Feng, J., 2014. Prismatic tensegrity structures with additional cables: Integral symmetric states of self-stress and cable-controlled reconfiguration procedure. International Journal of Solids and Structures 51 (25-26), 4294–4306.
URL http://dx.doi.org/10.1016/j.ijsolstr.2014.08.014

Zuk, W., 1968. Kinetic structures. Civil Engineering 38 (12), 62.